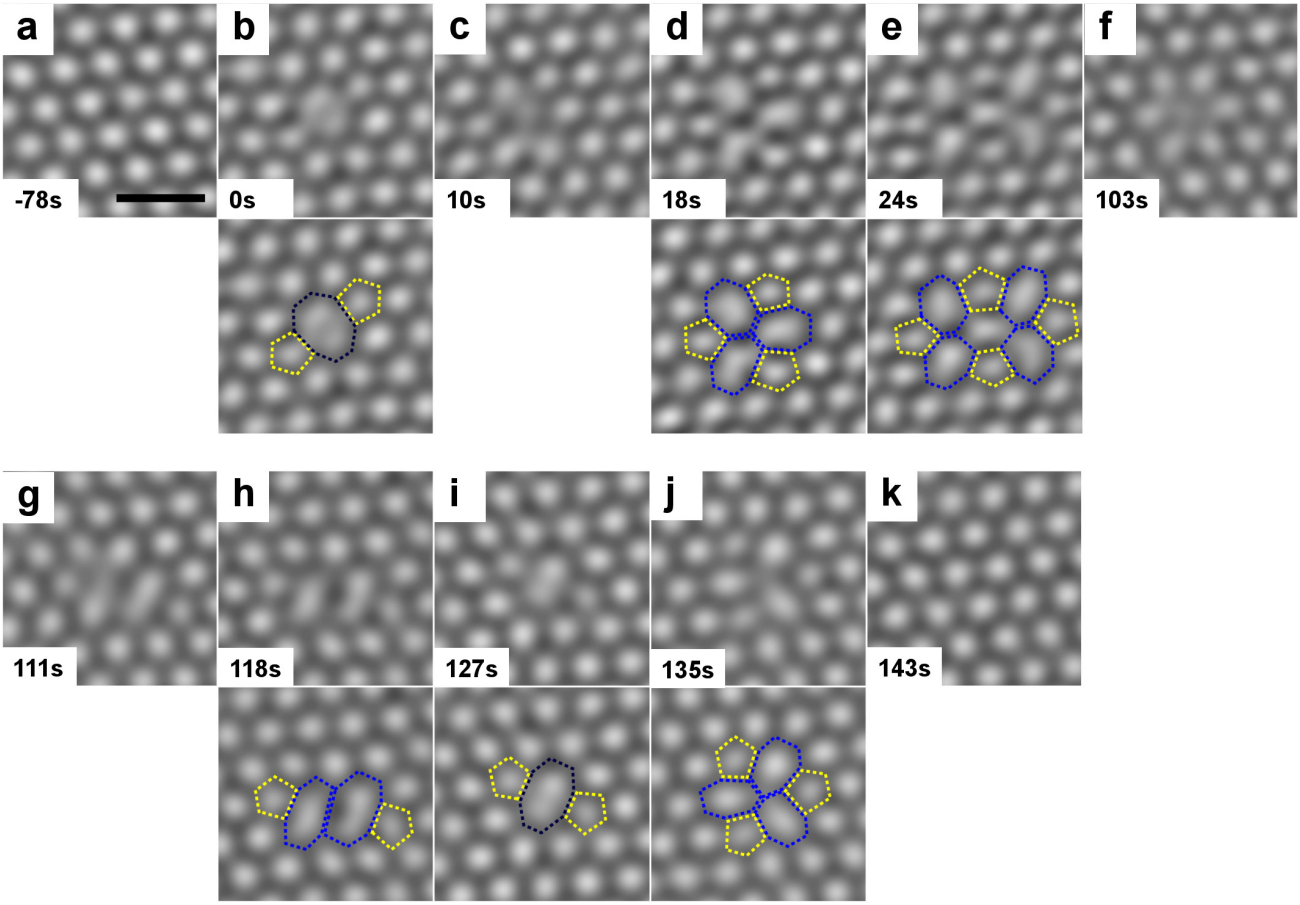

Supplementary figure S8: Time series for Stone-Wales (SW) rotations in a divacancy. Aberration-corrected transmission electron microscope (AC-TEM) time series showing the evolution of the same divacancy defect under continuous irradiation by the electron beam (imaging beam current density), demonstrating how readily divacancies can fluctuate between particular meta stable configurations over time scales that are relatively short (~ 1 second) compared to the time scale between defect formation and defect imaging (~ 30 seconds). As such an average defect parameterising value of 6 was used for characterising divacancies for the graph shown in figure 4a of the main text. The insert numbers denote the time, in seconds, relative to the first defect image. (a) Pristine graphene lattice before irradiation. (b) Divacancy formed by 30 s exposure to the focussed electron beam, imaged after astigmatism correction. (c) Blurring of the image; indicative of a bond rotation and reconfiguration in progress during the exposure. (d) A divacancy having undergone a SW bond rotation. (e) The same divacancy shifted through another SW bond rotation. (f,g) Further bond reconfigurations in progress. (h) The divacancy reconfigured into a dislocation dipole/twin monovacancies. (i) Reformed back into a divacancy, rotated to along a different armchair axis to that shown in (b). (j) The divacancy having undergone a SW bond rotation, as in (d) but directed along a different lattice plane. (k) The divacancy quenched back to a pristine graphene lattice. Panels with highlighted bonds are shown beneath (b,d,e,h-j); the non-transient states. The colour scheme denotes the number of carbons in the respective carbon ring, such that yellow, blue and dark blue represent 5-, 7- and 8-membered carbon rings, respectively. Scale bar denotes 0.5 nm.

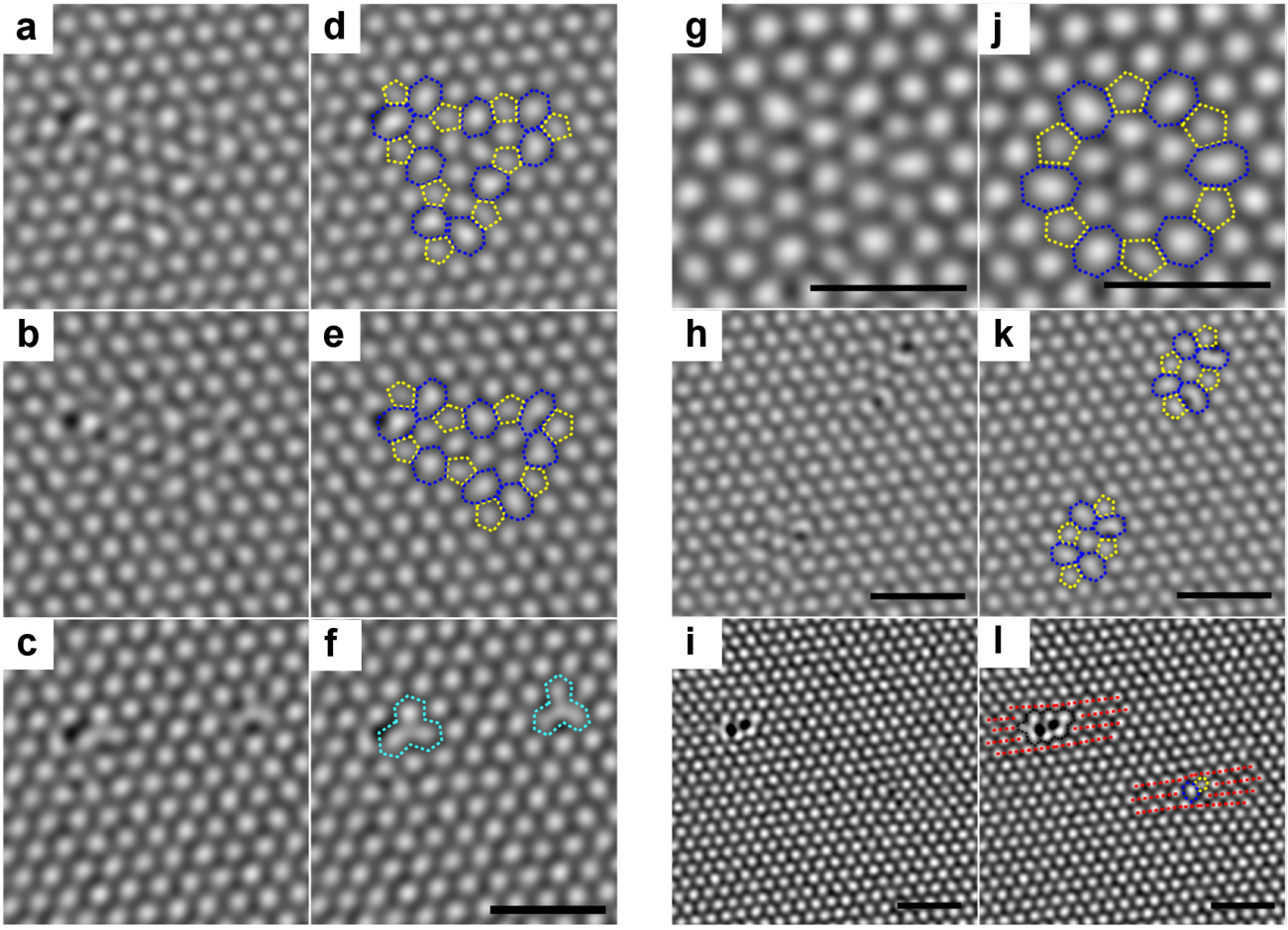

Supplementary figure S9: Defect stability. (a-c) Aberration-corrected transmission electron microscope (AC-TEM) images of the relaxation of a defect, as in figure 5 of the main text. (d-f) Annotated versions of (a-c). (g-i) AC-TEM images demonstrating defect stability, as in figure 5. (j-l) Annotated images of (g-i). Surface adatoms in (a-c,h,i) can be clearly resolved on the defects as spots of dark contrast. Scale bars denote 1 nm. The colour scheme denotes the number of carbons in the respective carbon ring, such that yellow and blue represent 5- and 7-membered carbon rings, respectively. Light blue in (f) highlights the monovacancy and the dashed red lines in (l) are along the lattice planes, to emphasise the dislocations. Scale bars denote 1 nm.

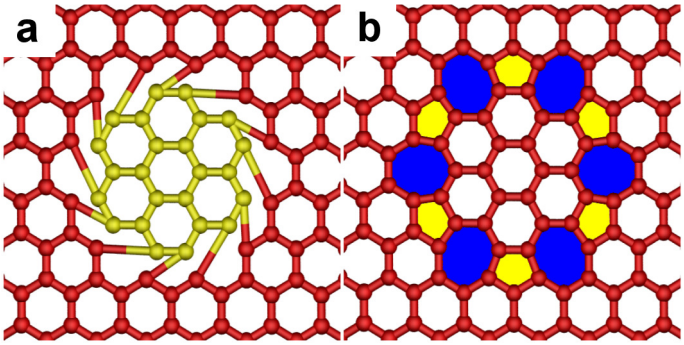

Supplementary figure S10: Atomistic model illustrating the closed-loop defect. Schematic models showing how the 5-7 closed loop structure is configured. The core of the defect, the seven 6-membered rings highlighted in (a), is rotationally misaligned by 30° with respect to the bulk lattice, with the bonds constructed as shown in (b). The colour scheme denotes the number of carbons in the respective carbon ring, such that yellow represents 5- and blue 7-membered carbon rings, respectively.

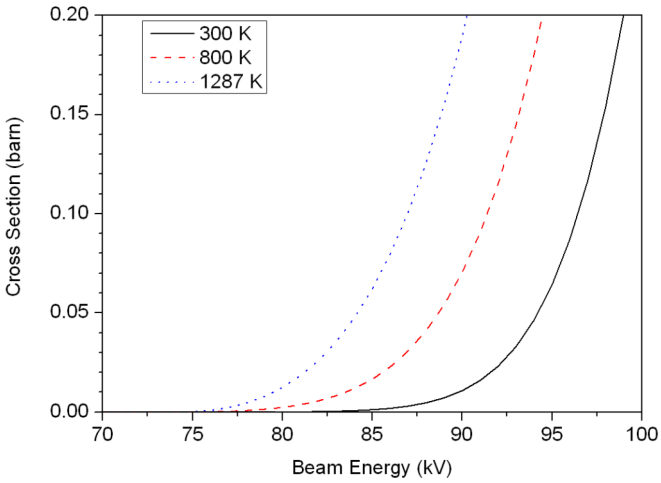

Supplementary figure S11: The dependence of carbon displacement cross section on electron beam energy. The carbon atom displacement cross section versus electron beam energy at temperatures of 300, 800 and 1287 K (the Debye temperature). At 80 kV cross sections of $\sigma_d(300\ K) = 7\times10^{-5}$ b, $\sigma_d(800\ K) = 2.4\times10^{-3}$ b and $\sigma_d(1287\ K) = 1.2\times10^{-2}$ b are expected.

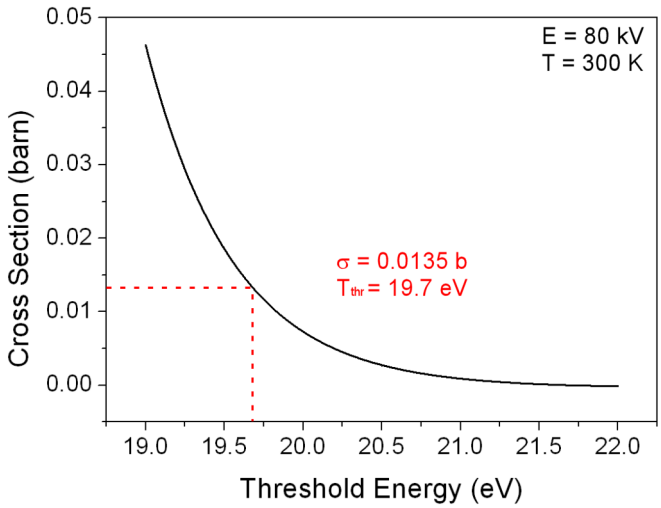

Supplementary figure S12: Sputtering cross-section as a function of threshold energy for sputtering. At 300 K and for 80 keV incident electrons a threshold energy for carbon sputtering in a collision of 19.7 eV leads to our observed cross-section of 1.35×10^{-2} barn.

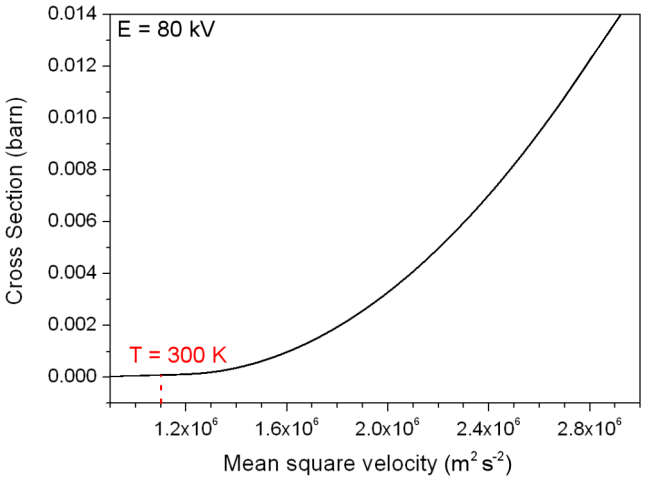

Supplementary figure S13: Sputtering cross-section as a function of mean-square-velocity. A plot showing the dependence of sputtering cross section on mean square velocity, calculated with 80 keV incident electrons. Marked is the expected mean square velocity at 300 K.

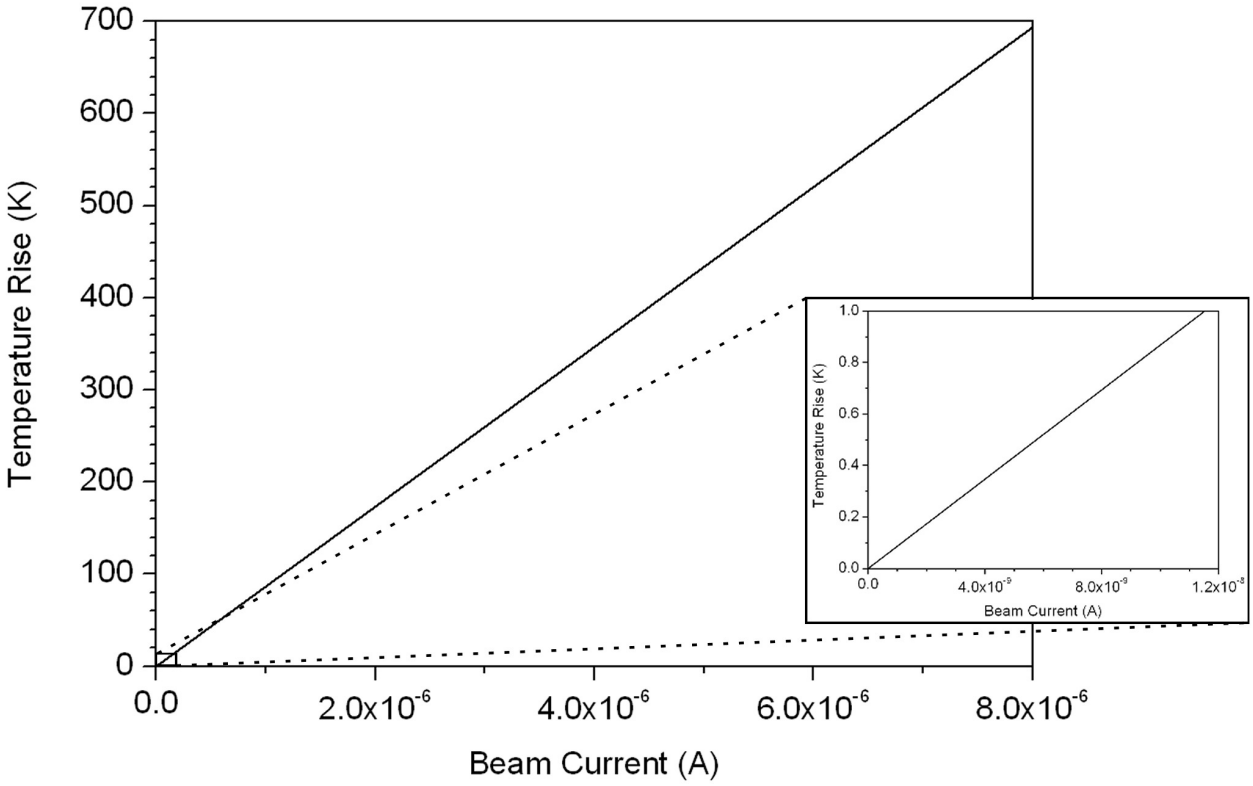

Supplementary figure S14: Quantification of electron beam induced sample heating. The effect of beam current on sample temperature, with the sample modelled as a monolayer of graphite and values of thickness 3.2 Å, thermal conductivity 4×10^3 $Wm^{-1}K^{-1}$, beam diameter 8 nm, inelastic mean free path 0.4×10^{-10} m and distance to heat sink of 1 µm used in modelling the temperature change.